The Hematite (α-Fe_2O_3) (0001) Surface: Evidence for Domains of Distinct Chemistry

X.-G. Wang, W. Weiss, Sh. K. Shaikhutdinov, M. Ritter, M. Petersen, F. Wagner, R. Schlögl, and M. Scheffler

Fritz-Haber-Institut der Max-Planck-Gesellschaft, Faradayweg 4-6, D-14195 Berlin-Dahlem, Germany

(Received 11 March 1998)

Using spin-density functional theory we investigated various possible structures of the hematite (0001) surface. Depending on the ambient oxygen partial pressure, two geometries are found to be particularly stable under thermal equilibrium: one being terminated by iron and the other by oxygen. Both exhibit huge surface relaxations (-57% for the Fe and -79% for the O termination) with important consequences for the surface electronic and magnetic properties. With scanning tunneling microscopy we observe two different surface terminations coexisting on single crystalline α-Fe_2O_3 (0001) films, which were prepared in high oxygen pressures. [S0031-9007(98)06733-7]

PACS numbers: 68.35.Bs, 61.16.Ch, 68.35.Md, 71.15.Ap

Although metal-oxide surfaces play a crucial role for several profitable processes, good quality experimental and theoretical studies of their atomic structure and electronic properties are scarce. For example, α-Fe_2O_3 appears to be the active catalytic material for producing styrene, [1], which was substantiated by recent reactivity studies performed over single crystalline hematite model catalyst films [2]. Other candidate applications are photoelectrodes [3] and nonlinear optics materials [4]. Nevertheless, the surface properties of α-Fe_2O_3 are basically unknown, and also for other metal oxides an understanding is only badly developed. The reason is the difficult preparation of clean surfaces with defined structures and stoichiometries, which, as in the case of hematite, can require high oxygen pressures not suitable in standard ultrahigh vacuum systems. Furthermore, electron spectroscopy techniques and scanning tunneling microscopy (STM) are hampered by the insulating nature of the material. We also note that surface-science techniques often do not probe a thermal equilibrium geometry but a frozen-in metastable state. Theoretical studies, on the other hand, have to deal with $3d$ electrons, oxygen with very localized wave functions, a rather open structure, unusual hybridization of wave functions, huge atomic relaxations, big super cells, and magnetism. This renders an *ab initio* study of α-Fe_2O_3 surfaces a most challenging investigation. Some theoretical studies of the geometry of α-Fe_2O_3(0001) have been performed using empirical (classical) potentials [5,6], and Armelao *et al.* [7] studied the electronic structure employing a cluster approach. In this paper we report spin-density functional theory calculations for a slab geometry (see Fig. 1). We use the generalized gradient approximation [8] for the exchange-correlation functional and the full-potential linearized augmented plane wave (FP-LAPW) method [9,10] to solve the Kohn-Sham equations. The STM study was performed on a thin hematite film grown epitaxially onto a Pt(111) substrate.

The identification of thermal equilibrium structures of surfaces is a prerequisite for an understanding of the endurance, electronic, magnetic, and chemical properties of the material. For a two-component material, such as Fe_2O_3, under realistic conditions the surface will exchange atoms with chemical reservoirs. Therefore we will analyze the Gibbs free energy with its dependence on the chemical potentials of the two components. For metal oxides, it is obvious that the O_2 partial pressure is the practical handle on this dependence. Interestingly, neither experimental nor theoretical studies have identified the composition and structure of surfaces of Fe_2O_3 so far, and it is unknown how the surface structure depends on the oxygen chemical potential. In this paper we show that the surface properties change significantly with O_2 pressure and that under typical oxygen pressure conditions, two chemically distinct domains are likely to exist.

The α-Fe_2O_3 crystallizes in the hexagonal corundum structure, where the primitive bulk unit cell contains six formula units (30 atoms). Along the [0001] axis this structure can be viewed as a stack of Fe and O_3 layers: ... Fe-Fe-O_3-Fe-Fe-O_3 .... The (0001) surface is stable and often occurs on naturally grown crystals [11]. It exhibits an unreconstructed (1×1) surface with a hexagonal unit cell [12,13]. In the total-energy calculations we considered the following (likely) surface terminations with (1×1) periodicity: Fe-Fe-O_3-..., Fe-O_3-Fe-..., O_3-Fe-Fe-..., O_2-Fe-Fe-..., O_1-Fe-Fe-..., where the latter two surfaces correspond to an oxygen termination with oxygen vacancies. For the Fe-O_3-Fe-... terminations we considered all four possible geometries of the surface Fe,

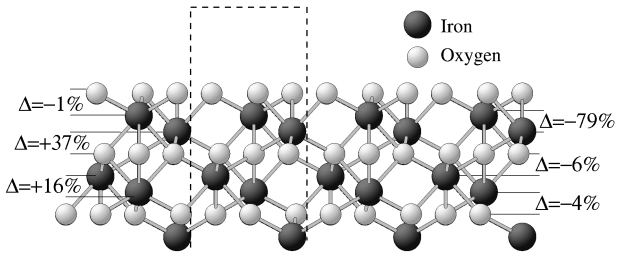

FIG. 1. Upper half of the slab for the unrelaxed O_3-terminated surface. The cross section of the upper half of the supercell is noted by the dashed rectangle. The Δ indicate the calculated interlayer relaxations in percent relative to an unrelaxed surface, i.e., a truncated bulk geometry.

 0031-9007/98/81(5)/1038(4)$15.00

and found that the energetically favorable surface is that with the top Fe site occupied according to the bulk stacking sequence. Figure 1 shows as an example our slab for the O_3-Fe-Fe-... surface study. We find that two of the five candidates considered have a particularly low energy and predict that both should be present under typical experimental conditions. These are the Fe-O_3-Fe-... and the O_3-Fe-Fe-... structures. The low energy of the Fe-O_3-Fe-... surface is consistent with recent findings for other corundum-type materials (Al_2O_3 [14] and Cr_2O_3 [15]), but for Fe_2O_3 it has not been identified so far. The other structure which we predict, i.e., the termination by O_3, is unexpected in general (also for other corundum-type crystals) because this termination suggests a high surface dipole moment and thus an electrostatically unfavorable situation. In fact, our calculations reveal that this argument, which is based on the understanding of the bulk properties of Fe_2O_3, is too simple for describing the surface. Indeed, both low-energy surface structures are stabilized by a significant surface relaxation which implies that the surface should be viewed as a "new material," not just a truncated bulk.

For the FP-LAPW calculations we use a kinetic-energy cutoff for the plane wave basis of $E_{\max}^{\mathrm{wf}} = 18$ Ry. This is a rather high value and makes the calculations very involved. However, because of the huge surface relaxations found in the course of this study we had to use rather small muffin-tin spheres ($R_{\mathrm{Fe}}^{\mathrm{MT}} = 0.95$ Å, $R_{\mathrm{O}}^{\mathrm{MT}} = 0.74$ Å) and therefore a large value for $E_{\max}^{\mathrm{wf}}$ was mandatory to ensure good numerical accuracy. Details of the calculations are presented elsewhere. The bulk as well as the surface calculations were performed with a hexagonal unit cell and a uniform $\mathbf{k}$-point mesh with five points in the irreducible part of the Brillouin zone. All parameters defining the numerical accuracy of the calculations were carefully tested. For the bulk we obtain the following results (experimental values [16] in parentheses): $a_0 = 5.025$ (5.035) Å, $c_0 = 13.671$ (13.747) Å, $z(\mathrm{Fe}) = 0.357$ (0.355) Å, $x(\mathrm{O}) = 0.308$ (0.306) Å. Our calculations give an antiferromagnetic ordering with a local moment of $M = 3.39\mu_{\mathrm{B}}$ (considering the contribution from the muffin tin only). The spins are pointing parallel to [0001], and in the Fe-Fe double layers are aligned parallel. But between neighboring double layers (separated by an O_3 layer) the spins are antiparallel. Our result is similar to recent bulk calculations using the augmented spherical wave method [17], but the magnetic moments are smaller than the experimental values $M = (4.6\text{–}4.9)\mu_{\mathrm{B}}$ [18,19]. This difference was blamed on difficulties with the experimental analysis [17,20]. The heat of formation per a Fe_2O_3 unit is 8.024 (8.48) eV [21]. The slabs consist of six O_3 layers and ten, twelve, or fourteen Fe layers, depending on the surface termination to be studied (see Fig. 1 as one example). All atoms of the slab are allowed to relax and no symmetry restrictions are applied. The antiferromagnetic ordering is found to remain up to the surface.

The Gibbs free energy Ω of the slab at temperature T and partial pressure p is given by

$$\Omega = E^{\mathrm{tot}} + pV - TS - \mu_{\mathrm{Fe}} N_{\mathrm{Fe}} - \mu_{\mathrm{O}} N_{\mathrm{O}}, \quad (1)$$

where E^{tot} is the total energy of the slab, μ_{Fe} the chemical potential of iron, and μ_{O} the chemical potential of oxygen. N_{Fe} and N_{O} are the number of iron and oxygen atoms of the supercell. For typical pressure and temperature, the pV and TS terms in Eq. (1) can be neglected. The Fe and O chemical potential are not independent, because they are related to each other by the existence of the Fe_2O_3 bulk phase. This gives

$$\Omega = E^{\mathrm{tot}} - \tfrac{1}{2} N_{\mathrm{Fe}} \mu_{\mathrm{Fe_2O_3(bulk)}} + (\tfrac{3}{2} N_{\mathrm{Fe}} - N_{\mathrm{O}})\mu_{\mathrm{O}}, \quad (2)$$

where $\mu_{\mathrm{Fe_2O_3}}(\mathrm{bulk})$ is the total energy per bulk Fe_2O_3 formula unit (with 2 Fe and 3 O atoms).

In Fig. 2 we show our results of Eq. (2) for various (1×1) geometries, where γ is the Gibbs free energy per surface area. The meaningful range of μ_{O}-μ_{O}(gas) is limited by the conditions that the chemical potential of Fe has to be smaller than that of an atom of bulk iron, and the chemical potential of oxygen has to be smaller than that of an oxygen atom of O_2. Otherwise an iron or oxygen condensate will form at the surface. The allowed range of the oxygen chemical potential, μ_{O}-μ_{O}(gas), is marked in Fig. 2 by the vertical dotted lines.

The results show that the Fe and the O_3-terminated surfaces are particularly stable. The relaxation energy is significant, in particular, for the O_3 termination. In fact, from these results we predict that under typical experimental conditions the surface should consist of two domains,

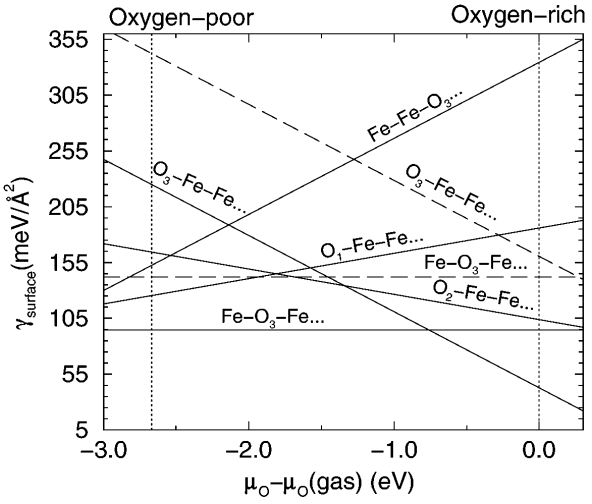

FIG. 2. Surface energies of different $Fe_2O_3(0001)$ surface terminations. μ_{O}(gas) is the chemical potential per oxygen atom of molecular O_2. The allowed range of μ_{O}-μ_{O}(gas) is indicated by the vertical dotted lines, where the left one corresponds to strongly Fe-rich (i.e., oxygen-poor) conditions, and the right one corresponds to strongly oxygen-rich conditions (i.e., high oxygen gas pressure). Solid lines show results for relaxed geometries, and dashed lines give, for comparison, results for unrelaxed surfaces.

with these two structures. The O_3 termination has not been discussed before but, for the Fe-O_3-Fe-... termination, semiempirical studies have been performed. Our surface energy for the relaxed geometry is 1.52 J/m^2 = 94.58 meV/Å which is in close agreement with the semiempirical studies of Mackrodt *et al.* [5], who obtained 1.53 J/m^2, and Wasserman *et al.* [6], who obtained 1.65 J/m^2. Also, other corundum-type materials have a comparable surface energy for the (0001) surface: For α-Al_2O_3 Manassidis *et al.* [22] obtained 1.76 J/m^2, and Rohr *et al.* [15] obtained for Cr_2O_3 a value of 1.60 J/m^2.

Table I collects the calculated surface relaxations for the Fe-terminated surface. We obtain a relaxation pattern which alternates when going away from the surface. For the Fe-terminated surface, the comparison with previous (semiempirical) studies reveals that a model using static ions [5] is not appropriate but, when some polarization is allowed [6], the system is apparently well described. In fact, our calculation shows that at the surface the covalent contribution to bonding is enhanced, which is mainly due to a hybridization of O $2p$ and Fe $3d$ orbitals. The work function of the Fe-terminated surface is calculated as 4.3 eV (before relaxation it is only 3.1 eV). Recently, in a LEED analysis for Cr_2O_3, Rohr *et al.* [15] determined a 60% reduction for the first Cr-O_3 interlayer distance, which is in surprisingly close agreement with our result for Fe_2O_3 (we obtain 57%). A detailed list of the geometry data which we obtained will be given elsewhere. Here, we note only that the O_3 triangles of the first oxygen layer, i.e., the second layer from the surface, exhibit a clockwise rotation by 2° without breaking the C_3 surface symmetry. No LEED analysis for the Fe-terminated (0001) surface of Fe_2O_3 exists so far.

The O_3-terminated surface (see Figs. 1 and 2) is indeed a very unexpected system and only stabilized by huge and unusual relaxations which are collected in Table I. The top layer O_3 triangles undergo a significant rotation (by 10°) without breaking the C_3 surface symmetry. The oxygen atoms remain nearly planar. Similar to the Fe-terminated surface, a very notable feature is the contraction of the first subsurface Fe-Fe interlayer spacing, followed by an expansion of the next Fe-O_3 spacing. The huge interlayer relaxations and the O_3 rotational reconstruction provide the important contribution to the decrease of the surface energy and stabilize the O_3-terminated surface. As mentioned above, the stability of this surface cannot be understood in terms of a simple ionic model, in which the surface oxygen atoms were negatively charged. Indeed, according to our calculations the ionic character of the O atoms is decreased at the O_3-terminated surface, and the covalent interaction between O $2p$ and Fe $3d$ states is enhanced significantly. This is also reflected in a noticeable *decrease* of the work function upon relaxation (from 8.3 to 7.6 eV).

TABLE I. Interlayer relaxations at the Fe-O_3-... and O_3-Fe-... surface relative to the corresponding bulk spacings.

Interlayer		Fe-O_3-... Present	Ref. [5]	Ref. [6]	Interlayer	O_3-Fe-... Present
Fe-O_3	1-2	−57%	+1%	−49%		
O_3-Fe	2-3	+7%	+5%	−3%	1-2	−1%
Fe-Fe	3-4	−33%	−47%	−41%	2-3	−79%
Fe-O_3	4-5	+15%	+20%	+21%	3-4	+37%
O_3-Fe	5-6	+5%	+3%	–	4-5	−6%
Fe-Fe	6-7	−3%	+2%	–	5-6	+16%
Fe-O_3	7-8	+1%	–	–	6-7	−4%
O_3-Fe	8-9	+4%	–	–	7-8	+4%

The surface relaxations and change in the nature of bonding at the surface goes hand in hand with a dramatic change in the magnetic properties. Here, we discuss the integral over the magnetization density considering the contribution from inside the muffin-tin spheres. Therefore the direct values should not be taken too literally. But differences in moments between different layers and between the relaxed and unrelaxed situation are indeed meaningful. For the Fe-terminated surface we find that the magnetic moment of the topmost Fe layer is reduced against the bulk value by about 7% (namely, $\Delta M = -0.24\mu_B$).

The electronic and magnetic properties of the O_3-terminated surface are unprecedented. We find that the subsurface iron layers change their character significantly. The local magnetic moments of the first and second Fe layer are reduced to less than 50% of the bulk values ($\Delta M = -1.79\mu_B$ and $-1.75\mu_B$, respectively), and, again, a significant fraction of this reduction occurs only upon surface relaxation and reconstruction. Interestingly, also the top O_3 layer now attains a noticeable magnetic moment ($M = 0.20\mu_B$ per atom). In the bulk, the magnetic moment of oxygen atoms is zero. Our calculations show that the surface states for the O_3-terminated surface are of Fe $3d$ character. They are partially occupied by the Fe $3d$ electrons formerly with different spin, which results in the decrease of the local magnetic moments of the iron atoms. Our calculations also show that the surface state electrons of the iron atoms reaching through the topmost O layer may noticeably affect the surface reactivity. Because of the high localization of the surface state the surface is predicted to be nonmetallic.

The STM experiments were performed in an ultrahigh vacuum system described in detail elsewhere [23]. It is equipped with a sample transfer mechanism and a separate preparation chamber for performing high pressure oxidation treatments. Single crystalline α-Fe_2O_3(0001) films were grown on a clean Pt(111) substrate surface. In a first step about 10 nm thick Fe_3O_4(111) magnetite films were prepared by repeated deposition of iron and subsequent oxidation for 2 min at temperatures at about 950 K in 10^{-6} mbar oxygen partial pressure [24]. Then, a final oxidation at $T = 1100$ K in 10^{-3} mbar oxygen partial pressure was performed for 10 min. The structure formed under these conditions was quenched by cooling down the sample to room temperature in the oxygen atmosphere. The oxygen was then pumped off and the sample was transferred back into the analysis chamber

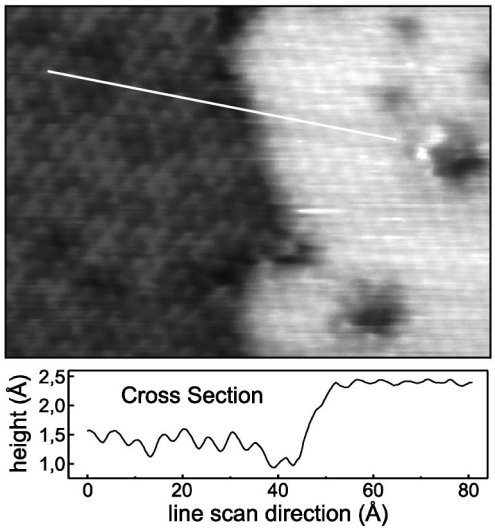

FIG. 3. Constant current image of an α-$Fe_2O_3(0001)$ surface prepared in 10^{-3} mbar oxygen partial pressure over an area of 100×80 Å^2 ($U = +1.3$ V, $I = 1.3$ nA. A cross section along the white line in the image is shown. Two different surface terminations can be seen.

and immediately studied by STM. These films exhibited no auger contamination signals and sharp (1×1) LEED patterns [12]. X-ray photoemission spectroscopy revealed only Fe^{3+} and no Fe^{2+} species, indicating the formation of a single phase hematite film [13].

Figure 3 shows an atomic resolution STM image of the α-$Fe_2O_3(0001)$ surface. A dark region and a bright region can be seen. They both exhibit hexagonal lattices formed by atomic protrusions with a periodicity of 5 Å, which corresponds to the interatomic distance within the (0001) Fe planes of the α-Fe_2O_3 structure. Below, a cross section along the white line in the STM image is shown, which displays the 5 Å periodicity and the two regions separated by a step about 1 Å high. This step height considerably deviates from the distance between two equivalent (0001) surface terminations of α-Fe_2O_3, which are separated by a monoatomic step with a height of 2.28 Å. We always measure monoatomic steps or multiples of them between equivalent regions on the hematite surface. Therefore the two regions in Fig. 3 correspond to two different surface terminations that coexist on the α-$Fe_2O_3(0001)$ surface. This is further substantiated by their different corrugation amplitudes depicted in the cross section plot in Fig. 3, which are 0.1 and 0.2–0.3 Å. Based on the apparent topographic height difference measured with the STM, we interpret the bright region as the Fe-terminated and the dark region as the O-terminated surface. About 20% of the entire sample surface is covered by the bright termination as determined by numerous large-area scans. They form islands preferentially located near step edges on top of the dark termination, with sizes ranging between 20 and 200 Å. We also confirmed that their formation depends on the oxygen partial pressure during the preparation (compose the discussion of Fig. 2 above). Measurements of STM spectroscopy, work function, etc., and a detailed analysis of the dependence on oxygen pressure are in progress.

In summary, we have presented a detailed *ab initio* FP-LAPW study of the stoichiometry and structural relaxations of the α-Fe_2O_3 (hematite) (0001) surface. The calculations predict two types of surfaces [thermal equilibrium with (1×1) symmetry], which depend on the growth conditions. We find a large inward relaxation of the first layer for the Fe-terminated surface and a huge contraction of the interlayer spacing between the Fe subsurface layers for the O_3-terminated surface. In addition to the relaxations along the [0001] direction, the O layers of both surfaces have a plane rotational reconstruction. To our knowledge, this is the first finding for these types of special relaxations and plane reconstruction of oxygen layers at a metal-oxide surface. We also predict an unusual electronic structure of the O_3-terminated surface with a noticeable presence of states from the subsurface Fe layer. This also results in a magnetic polarization of the oxygen. With STM we confirm the existence of two different surface terminations coexisting on single crystalline hematite (0001) films, which have been prepared under a high oxygen pressure of 10^{-3} mbar.

[1] T. Hirano, Appl. Catal. **26**, 65 (1986).
[2] W. Weiss *et al.*, Catal. Lett. **52**, 215 (1998).
[3] L. L. Hu and T. Yoko *et al.*, Thin Solid Films **219**, 18 (1992).
[4] T. Hashimoto *et al.*, J. Ceram. Soc. Jpn. **101**, 64 (1993).
[5] W. C. Mackrodt. *et al.*, J. Cryst. Growth **80**, 441 (1987).
[6] E. Wasserman *et al.*, Surf. Sci. **385**, 217 (1997).
[7] L. Armelao *et al.*, J. Phys. Condens. Matter **7**, L299 (1995).
[8] J. P. Perdew *et al.*, Phys. Rev. B **46**, 6671 (1992).
[9] P. Blaha *et al.*, Comput. Phys. Commun. **59**, 399 (1990).
[10] B. Kohler *et al.*, Comput. Phys. Commun. **94**, 31 (1996).
[11] *The Iron Oxides*, edited by R. M. Cornell *et al.* (VCH, New York, 1996).
[12] W. Weiss, Surf. Sci. **377-379**, 943 (1997).
[13] Th. Schedel-Niedrig *et al.*, Phys. Rev. B **52**, 17 449 (1995).
[14] J. Guo *et al.*, Phys. Rev. B **45**, 13 647 (1992).
[15] F. Rohr *et al.*, Surf. Sci. **372**, L291 (1997).
[16] L. W. Finger *et al.*, J. Appl. Phys. **51**, 5362 (1980).
[17] L. M. Sandratskii *et al.*, J. Phys. Condens. Matter **8**, 983 (1996).
[18] J. M. D. Coey *et al.*, J. Phys. C **4**, 2386 (1971).
[19] E. Kren *et al.*, Phys. Lett. **19**, 103 (1965).
[20] D. D. Sarma *et al.*, Phys. Rev. Lett. **75**, 1126 (1995).
[21] *CRC Handbook of Chemistry and Physics*, edited by R. C. Weast (CRC Press, Boca Raton, Florida, 1987), 67th ed.
[22] I. Manassidis *et al.*, Surf. Sci. Lett. **285**, L517 (1993).
[23] W. Weiss *et al.*, J. Vac. Sci. Technol. A **16**, 21 (1998).
[24] W. Weiss *et al.*, Phys. Rev. Lett. **71**, 1848 (1993).